Nano Energy 75 (2020) 104975

Contents lists available at ScienceDirect

Nano Energy

journal homepage: http://www.elsevier.com/locate/nanoen

Power cables for triboelectric nanogenerator networks for large-scale blue energy harvesting

Guanlin Liu [a,b,c,1], Longfa Xiao [a,1], Chaoyu Chen [c], Wenlin Liu [b], Xianjie Pu [b], Zhiyi Wu [c], Chenguo Hu [b,*], Zhong Lin Wang [a,c,**]

[a] *Center on Nanoenergy Research, School of Physical Science and Technology, Guangxi University, Nanning, Guangxi, 530004, PR China*
[b] *Department of Applied Physics, State Key Laboratory of Power Transmission Equipment & System Security and New Technology, Chongqing University, Chongqing, 400044, PR China*
[c] *School of Material Science and Engineering, Georgia Institute of Technology, Atlanta, GA, 30332, USA*

ARTICLE INFO

Keywords:
Triboelectric nanogenerator
Power cable
Blue energy
Water wave

ABSTRACT

Triboelectric nanogenerators (TENGs), a prospective technology for large-scale harvesting of blue energy from the ocean, have been extensively investigated recently. However, little attention has been paid to the cables linking the individual TENG units to form an energy harvesting network. Herein, several basic requirements for power cables suitable for effective TENG networks are outlined. The cables should avoid tangling among the TENG units, protect the transmission wires, and output electric power. Here, a TENG network based on plane-like power cables consisting of spring steel tapes and three polymer films is described. The steel tape inside the power cables has a dual role as both structural skeleton and an electrode. The tape guarantees the stability of the TENG network and eliminates the electrostatic induction from ions in seawater. The porous PTFE film on the outside is highly hydrophobic and generates electricity by liquid-solid interface contact while collaborating with the steel tapes. The working mechanism and output performance of the power cable were systematically studied. A maximum open-circuit voltage of 34 V and a transferred charge quantity of 25 nC were achieved using a single cable in a single period. An over-water test was also carried out to experimentally demonstrate the feasibility of the TENG networks. This work provides a possible strategy for network construction for large-scale blue energy harvesting.

1. Introduction

The ocean carries enormous amounts of wave energy, enough to supply the electricity needs of humanity if converted into electricity [1–3]. At present, most of our electricity supply is generated by spinning turbines, which convert mechanical energy into electrical energy. Turbine technology based on electromagnetic induction is also applied to harvesting wave energy in the ocean [4]. However, water waves are not consistently strong, reducing turbine effectiveness. Therefore, new techniques other than turbines to capture energy from ocean waves are called for.

In 2012, Wang et al. invented a triboelectric nanogenerator (TENG) that combines triboelectric effects and electrostatic induction to convert mechanical energy into electricity [5,6]. Normally, two different materials hold opposite charges after contact with each other, producing a potential difference in nearby electrodes once they move relative to one another. This potential difference drives electron flow across the external circuit [7]. Due to its various advantages, TENG can harvest almost any form of mechanical motion energy, allowing numerous achievements in electricity generation and self-powered sensor design [8–14]. The instant power area density and conversion efficiency of TENGs can exceed 500 W/m^2 and 50%, respectively [6]. TENGs can be applied to microplasma emission [15], molecular mass spectrometry [16], washable multilayer air filters [17], self-powered microfluidic transport systems [18], and wireless power transmission [19,20]. Gathering blue energy from ocean waves, is a key priority for TENG technology [7,21]. Compared with electromagnetic generators based on turbines, TENGs are lightweight, low-cost and easy to fabricate, making

* Corresponding author.
** Corresponding author. Center on Nanoenergy Research, School of Physical Science and Technology, Guangxi University, Nanning, Guangxi, 530004, PR China.
E-mail addresses: hucg@cqu.edu.cn (C. Hu), zlwang@binn.cas.cn (Z.L. Wang).
[1] GL Liu and LF Xiao contributed equally to this work.

https://doi.org/10.1016/j.nanoen.2020.104975
Received 17 March 2020; Received in revised form 16 May 2020; Accepted 16 May 2020
Available online 13 June 2020

it a promising alternative for future blue energy technology. For the past several years, various TENG devices for blue energy harvesting have been designed, including spherical [22,23], cylindrical [24,25], cuboid or oblate spheroidal [26–29] TENGs, with various working modes including contact-separation [23,24,26,29], single electrode [30,31], and freestanding triboelectric-layer modes [25,28]. Each of these TENG designs has its own unique strategy to accommodate the corresponding mechanical triggering conditions.

As water waves exist on the surface layer of oceans, tens of thousands of TENG units must cover the sea surface to form large-scale arrays to harvest wave energy, as depicted in Fig. 1a. Effectively connecting these individual TENGs presents challenges. Previous works demonstrate groups of TENG units connected by flexible conducting wires, but under rough sea conditions, TENG units with flexible connections would easily tangle with each other [22,23]. No specialized investigation has focused on the connection of TENG units for blue energy harvesting. General technical requirements should be established for these connecting cables before integrating them with TENG units.

In this paper, we experimentally demonstrate the superiority of a specially designed cable over the commonly used wires described previously. Several basic requirements are outlined for this kind of power cable in building large-scale TENG arrays that work efficiently and consistently. First, the power cables should be rigid, to prevent tangling among TENG units. Second, the cables should protect the transmission wires from seawater erosion and interference. Third, it is desirable if the cables could themselves output electric power, since they are a large portion of the overall system. A power cable suitable for use with TENGs, consisting of two spring steel tapes and three polymer films, is illustrated in Fig. 1. This plane-shaped power cable design can limit horizontal motion among interconnected TENG units and prevent entanglement. The conducting wires, sandwiched between the two spring steel tapes, are protected from interference and corrosion by seawater. This cable design can also produce electricity when the power cable contacts and then separates with the water, further improving the output performance of the whole TENG network. The spring steel tapes inside the cable are anti-fatigue, highly resilient, and suitable for long-term operation. The effects of water interference on various transmission wires were experimentally compared, and the working mechanism and major influence factors on the output performance of power cable were systematically studied. A maximum voltage of 36 V and maximum transferred charge of 26 nC were achieved by a single power cable in one motion period. The water tank test also showed that the power cable described in this paper can work harmoniously with TENG units and meet the requirements proposed above. The structure design of the connecting device might not be perfect for all TENG networks, and the proposed requirements may not be mature, but this is a first step and more effort is needed to improve the application.

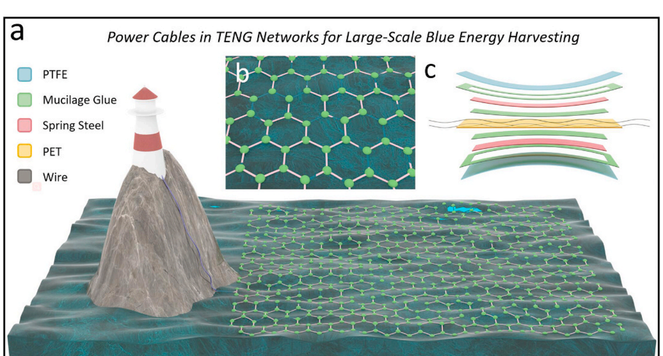

Fig. 1. a) Thousands of triboelectric nanogenerators connected by power cables for large-scale blue energy harvesting to power electrical devices in a lighthouse. b) Enlarged structure of a TENG array with honeycomb-like topology. c) Breakdown drawing of the power cable.

2. Results and discussion

2.1. Mechanical requirements of the power cable

The motion of a floating object on water can mainly be divided into four kinds: deflection, vertical motion, horizontal motion and rotation around the central axis. The rotation is too weak to be considered here, so the mechanical requirements focus on the other three kinds of motion. Large-scale TENG arrays for blue energy harvesting require restricted horizontal relative motion, to avoid entanglement under rough sea conditions. However, vertical motion and deflection should be free so that the TENG units can capture mechanical energy from the waves. This might suggests the use of a broad, flat 'plane-like' connecting device with flexural properties. As depicted in Fig. 1a, thousands of TENG units connected by plane-like power cables could form a large-scale array to provide electricity for isolated systems in the sea. As shown in Fig. 1b, the connection topology would form a honeycomb shape, with all TENG units on join points. This brings three benefits. First, the consumption of the power cables would be minimized, the ratio of TENG units to power cables would approach to 2:3 as the unit number increased. Second, as each TENG unit would have only three power cables to connect with, giving higher sensitivity to ocean waves with less constraint on the unit's motion. Third, the honeycomb-like connections would have high structural stability, keeping the array in shape against external forces. These features give a honeycomb connection topology advantages, compared with the chessboard shape commonly used.

Fig. 1c illustrates a power cable with a symmetrical structure composed of two spring steel tapes and three polymer films bound by mucilage glue. The PTFE films on the outside possess excellent mechanical properties and anti-corrosive qualities, and also serve as a frictional layer. The spring steel tapes inside have a well-polished surface, possess good elasticity, flatness, and fatigue-resistance, and act both as a skeleton and an electrode. The polyethylene terephthalate (PET) film in the middle is the same area as the PTFE films. The detailed fabrication process of power cable is discussed in the Experimental Section. Inside the power cable, room is reserved for transmission wires between the two steel tapes, since large TENG arrays may need such wires to transmit the output electricity. These design details can be adjusted according to specific operational needs. More features of power cable are discussed in the following sections. Conclusively, power cables meet the basic mechanical requirement, ensuring structural stability and high-response.

2.2. Shielding requirement

Without special power cables, the electricity transmission wires within a TENG array would be probably immersed in seawater directly. Electrostatic induction from ions in seawater then consumes power in the transmission wires [28]. To confirm this, a series of experiments was conducted to examine the influence of tap water and salt water on power transmission wires. A connect-separation mode TENG was fabricated and fixed on a linear motor. The TENG used a Cu/PTFE/Cu sandwich structure with an effective contact area of 4 cm × 4 cm. A linear motor applied linear reciprocating motion to the TENG, causing it to produce stable, continuous electricity. This was used to simulate the output of a TENG unit on the ocean. The parallel-plate TENG output 128 V of voltage, 72 nC of transferred charge per period, and 12 μA of short-circuit current at 2 Hz. The two electrodes of the TENG were connected to a variety of transmission wires, including enameled copper wires, Dupont lines, alligator clip lines, silver jacketed wires, and two enameled copper wires through the power cable, with open-circuit or short-circuit of two steel tapes. Using an acrylic holder, a 10 cm length of these wires could be immersed into water, as shown in Fig. 2a, and in Fig. S1 in the Supporting Information.

For each connection condition, all those transmission wires were tested in four different states: in air before immersion, during immersion in tap water, during immersion in salt water, and in the air after immersion. In each of these states, the output signals are measured individually as presented in Figs. S2–S4. The resulting normalized transferred charge and voltage are depicted in Fig. 2b. The transferred charge is nearly the same whether in air or water, and the short-circuit current, shown in Fig. S4, also keeps constant. However, the open-circuit voltage decreases during immersion. The voltage decreased by nearly 16% when the enameled copper wire was immersed in salt water due to its thin insulation. Since the alligator clip line had a thicker scarfskin than the Dupont line and silver jacketed wire (Fig. S5), it had a better shielding effect. The dampening effect of water on the immersing transmission wires might mainly attribute to the capacitive reactance between the power cable and water, which is related to the conductivity and dielectric constant of the water. In this case, the higher concentrations and ionic valency of the ions, the greater the influence of the water on the electricity, which might have less relationship with the ion types in the water. The enameled copper inside the power cable transmits the electrical signal efficiently with less than 2% loss, having the optimal shielding performance, which might be attributed to the spring steel tapes inside.

Without special protection, there is a further risk of transmission conducting wires losing their insulation and being exposed to water due to incident injuries in long-term operation. To explore the influence of water on bare transmission wires, three acrylic wire holders were used to run the same measurements as before on bare wires. This time, each holder held two paralleled enameled copper wires with a separation of 1 cm (Fig. S1c). In one of the holders (designated Holder #2), one wire was scraped to remove its insulation layer along a 1 cm length (Fig. S5). In Holder #3, both wires were similarly scraped; neither wire in Holder #1 was scraped.

The raw experimental data from this test are shown in Figs. S6–S8, and the concise result is displayed in Fig. 2c. The electric output using Holder #1 behaved similarly at different frequencies and had only small voltage losses when immersed. While the short circuit current and transfer charge using Holder #2 were the same as that of Holder #1, the voltage declines significantly during immersion. Predictably, the voltage loss in salt water was larger than that in tap water. When a conducting wire was exposed, electrons in the transmission wires tended to leak into the water, due to the resistance of electrometer in V gear approaching infinity relative to the rest of the circuit. A larger loss is received with a higher ion concentration. Thus, the loss associated with Holder #3 was elevated, compared with Holders #1 and #2. Although the short-circuit current was only slightly changed, the transferred charge quantity was found to decrease in salt water, except at 0.8 Hz. The waveform baseline of transferred charge also shifted, especially in salt water, as shown in Fig. S7, thus the readings are not accurate enough to reflect the actual amount. More importantly, the voltage fell to zero when two exposed wires were immersed in tap water or salt water. This is because the wires were short-circuited by the water, where the resistance was much lower than the input resistance of the electrometer. To understand the behavior of the transferred charge under various external resistances, we added a resistance box into the measuring circuit in series. The resulting waveform of the transferred charge is recorded in Fig. S9. For all holders, electron transfer slows gradually as the external resistance increased, resulting in more electron loss in water and a lower transferred charge quantity through the electrometer per unit time. This indicates, unsurprisingly that more electrons dissipate in water when two partially bare wires were exposed to water.

The above experimental results emphasize the importance of a well-insulated power cable and the hazard of bare transmission wires. Our proposed power cable design provides shelter for the wires, protects the insulation, and keeps the transmission wires away from the electrical interference of seawater.

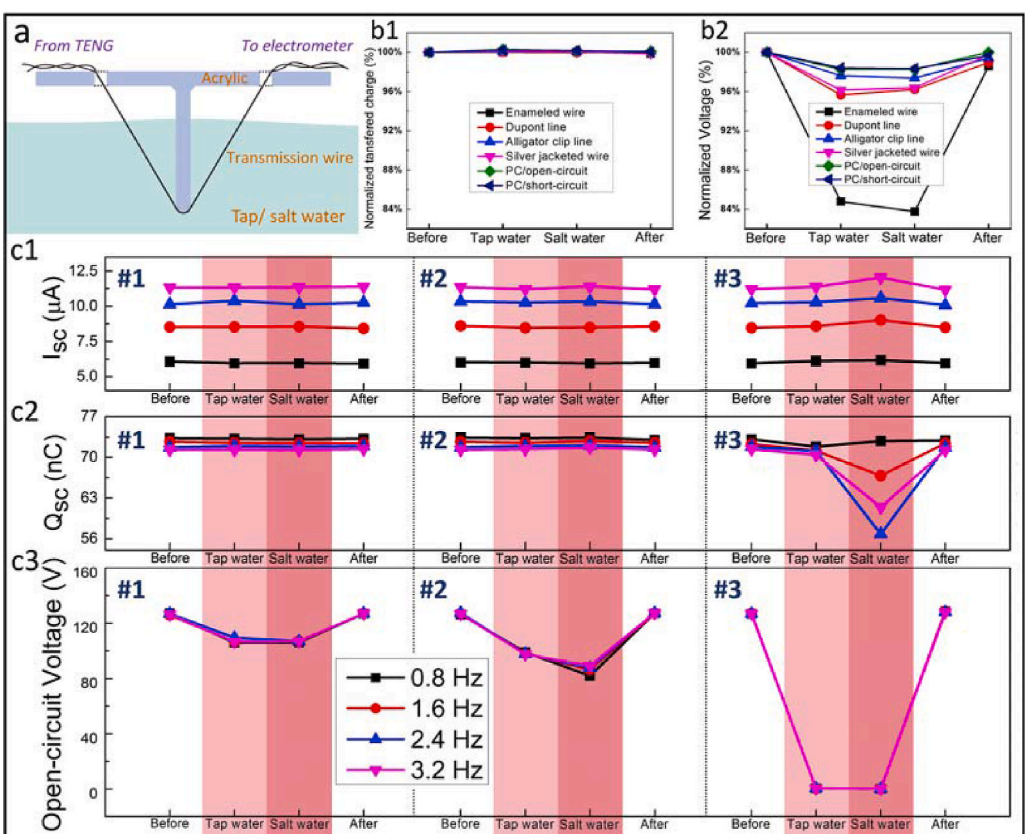

Fig. 2. The influence of water on different transmission wires carrying the electricity of a CS mode TENG. a) The 2D schematic of the experimental setup of the transmission wire part. Various transmission wires were used, with 10 cm immersed in tap/salt water using acrylic holders, with one end connected to the TENG and the other to a electrometer. b) Normalized short-circuit transferred charge quantity per cycle b1) and normalized open-circuit voltage b2) of the TENG with six different transmission wires under four different conditions: in the air before immersion, immersed in tap water, immersing in salt water, and in the air after immersion. c) Short-circuit current c1), short-circuit transferred charge quantity per cycle c2) and open-circuit voltage c3) of the TENG with three kinds of copper wires: #1 untreated, #2 one scraped wire, and #3 both wires scraped.

2.3. Electrical output and interface properties

In a large-scale TENG network, the number of power cables would greatly exceed the number of TENG units. It would be beneficial if the power cables themselves could also produce electricity. In the design discussed in this study, the two PTFE films on the power cable act as frictional layers that contact/separate with water as the power cable moves in and out of water, and two steel tapes serve as electrodes, allowing the cable itself to produce electricity. The working principle of the power cable is illustrated in Fig. 3a. Due to PTFE's high electronegativity [32], both PTFE films are negatively charged by the frequent contact with water. When water contacts the bottom of the cable, positive ions in the water are attracted by the negative charge on the surface of the PTFE film. The remaining negative charge on the top produce a potential difference between the two electrodes, which drives free electrons to flow from the top electrode to the bottom electrode, resulting in an upward current in the external circuit (state i). As the water level rises, contact between the top PTFE film and the water frees the electrons in bottom electrode, so they flow back to the top electrode, generating a reversed current (state ii). When the water level goes down (state iii), the negative charges on the top PTFE film repel the electrons on the top electrode once again, creating an upward current. As the water-level keeps going down, the power cable rises out of the water, and electrons go back to the top electrode, generating a downward current. The periodic movement of the power cable relative to the waves leads to cyclic contact and separation between the two PTFE films and water, which produces periodic electric output signals, as shown in Fig. 3b.

The hydrophobicity of the PTFE film is also important for the output performance of the power cable. Poor hydrophobicity would leave residual water on the films when the cable is out of the water. This incomplete separation between the film and water would reduce the electron transfer, and thus output. Thus, the materials selection and the surface topography are two vital factors for enhancing the output performance for nanogenerator [33,34] and the frictional layer used in the power cable is PTFE film with polyporous and highly hydrophobic. The material's contact angles with tap water and salt water are nearly equal, 122° and 124° respectively, as shown in Fig. 3c.

To find out the time influence of salt water on the surface of PTFE film, film samples were dipped in salt water for 3 h, then characterized by energy dispersive spectroscopy (EDS) and scanning electron microscopy (SEM) after gold spraying, as displayed in Fig. 3e and f. The SEM images suggest no changes on the PTFE surface after immersion in the salt water. No sodium or chlorine was detected by EDS, further confirming the absence of residual NaCl on the film.

The stress-strain curve of the cable was measured by bending the power cable in directions parallel and perpendicular to the plane of the cable, as shown in Fig. 3d. The cable was easily bent perpendicular to the plane, but difficult to bend along the plane. This can be used to prevent collisions of TENG units in an array, by minimizing horizontal motion.

To investigate the output response of the power cable under different external mechanical excitations, one end of the power cable was fixed at the surface of the water by an acrylic support, and the other end was connected to a rubber band and polyester thread. As presented in Fig. S10, the rubber band, whose other end was fixed to the floor of the water tank, pulled the power cable downward. The polyester thread, connected to the runner of a linear motor, pulled the power cable upward through a crown block. Therefore, the power cable was pulled in and out of the water with a period and amplitude the same as the movements of the linear motor. The influence of the motion frequency and amplitude on the output performance of the power cable was measured in tap water and salt water, as depicted in four color contour maps in Fig. 4, where all contour graphs are smoothed by a bilinear interpolation algorithm for ease of understanding. Each pair of 2D graphs in Fig. S11–S12 corresponds to a contour graph in Fig. 4 and exhibits the output performance under various conditions. In these figures, the output of the cable in tap water exhibits no monotonic change caused by the interaction of water wave and power cable. The maximum output voltage and transferred charge per cycle reach 34 V and 25 nC, respectively, for a motion period of 0.8 s with an amplitude of 3 cm in tap water. The waveforms of the output under different conditions are presented in Fig. S13. However, in salt water, the output voltage and transferred charge fall to 4.9 V and 3.4 nC, respectively, at a motion period of 0.8 s with an amplitude of 5 cm.

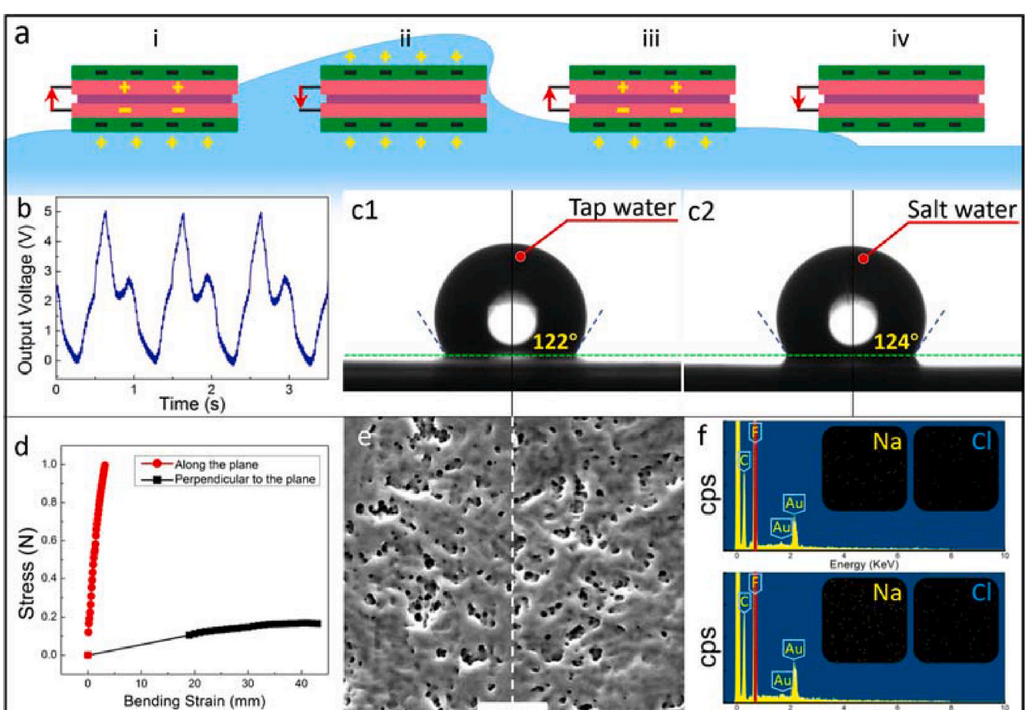

Fig. 3. a) Working principle of the power cable under water excitations and its b) typical output voltage waveform. The red arrows represent the direction of current. c) Contact angle of tap water c1) and salt water c2) measured on the PTFE film. d) Stress-strain curve of the power cable bending in two different directions. e) SEM images of the PTFE surface before (left half) and after (right half) immersion in salt water for 3 h. The scale bar is 5 μm. f) EDS results of the PTFE surface before (top) and after (bottom) immersion in salt water for 3 h.

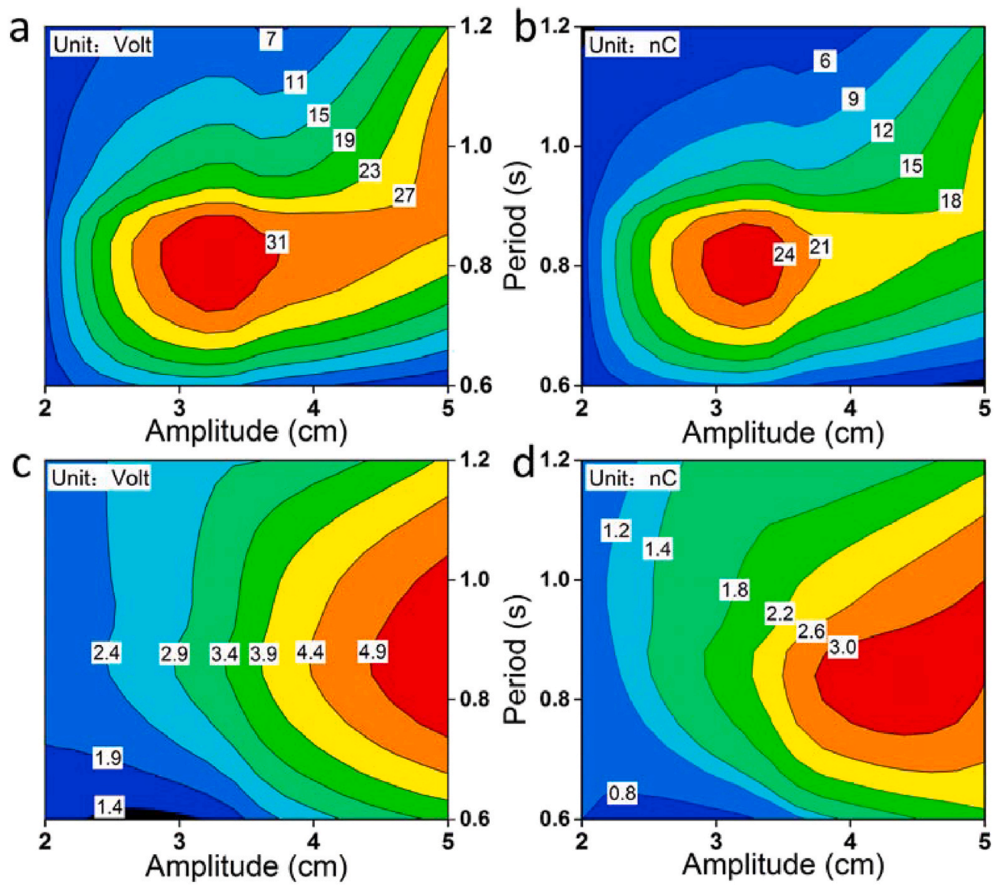

Fig. 4. Color contour graphs providing electrical characterization of a power cable under varied amplitude and motion periods. The graphs show the open-circuit voltage (a and c) and transferred charge quantity per cycle (b and d) in tap water (a and b) or salt water (c and d).

According to Nie's work, ions in salt water accumulate at the liquid-solid interface and hinder the electron transfer process due to the screening effect [35,36]. Since the negative charges are mostly accumulated by electron transfer, not ionic adsorption, the charge quantity on the PTFE surface in saltwater decreases, causing a decline in output performance. The output power for different resistive loads in both tap water and salt water under a motion period of 1.2 s and an amplitude of 5 cm are shown in Fig. S14. The calculated maximum peak power rose as high as 0.18 μW at 50 MΩ in tap water, and 0.13 μW at 70 MΩ in salt water. The maximum output power density of 90 $\mu W/m^2$ in tap water is obtained with the external resistance of 50 MΩ. Notably, realistic water waves will be somewhat randomized, and so the maximum voltage in field applications would not precisely match the data in Fig. 4. The output power can be improved by optimizing the design, careful material selection, or appropriate power management circuits.

2.4. Application demonstrations

With the characteristics outlined above, the power cable can in principle serve as a connecting device to link up TENG units in a large-scale array, protect transmission wires from sea conditions, and produce electricity at the same time. To test the viability of the cable, a small TENG array consisting of four oblate spheroidal shells connected by four power cables was fabricated to simulate one cell of large-scale array. As shown in Fig. 5a and Fig. S15, one of the four shells contained a steel plate based TENG that could produce electricity when excited by wave action. This TENG had two sets of output wires, one which exited its shell directly, and one which exited only after passing through all four power cables in a loop. The output voltage waveform acquired by the direct-exit set of wires is presented in Fig. 5b. Each of the other three shells contained a clump weight to adjust itself to the waterline, so that the power cable would touch the water properly. The TENGs used in these shells was similar to the upper part of the oblate spheroidal TENG (OS-TENG) described previously [29]. Each electrode in the power cables was connected to a bridge circuit individually, and then followed by a third set of transmission wires that also passed through power cables, as shown in Fig. 5a.

A water tank filled with tap water and a linear motor were used to produce water waves. Three rollers were placed on a flat floor to support the water tank, so that it could be pushed back and forth by the linear motor, with the runner fixed on the outer wall of the water tank. The linear motor operated with a motion period of 0.8 s and an amplitude of 3 cm. The TENG array swung as the waves moved. In addition to maintaining the rhomboid structure of the array, the power cable could also produce electricity, as shown in Fig. 5f. Importantly, the output electrical energy of the OS-TENG through the four power cables was protected well. No significant decline was found in Fig. 5d and e, emphasizing the shielding properties of the power cable in a practical scenario.

3. Conclusions

This work discusses a triboelectric nanogenerator-based power cable designed for connecting TENG units into a large-scale network. The steel-tape-based plane-like structure of the cable can keep TENG units in the network from colliding while allowing them relatively free deflection and vertical motion. The power cable provides an interference-free shelter for multiple transmission wires between its steel tapes. The PTFE films on the outside provide physical stability and high hydrophobicity to resist seawater erosion. They also serve as the frictional layer for

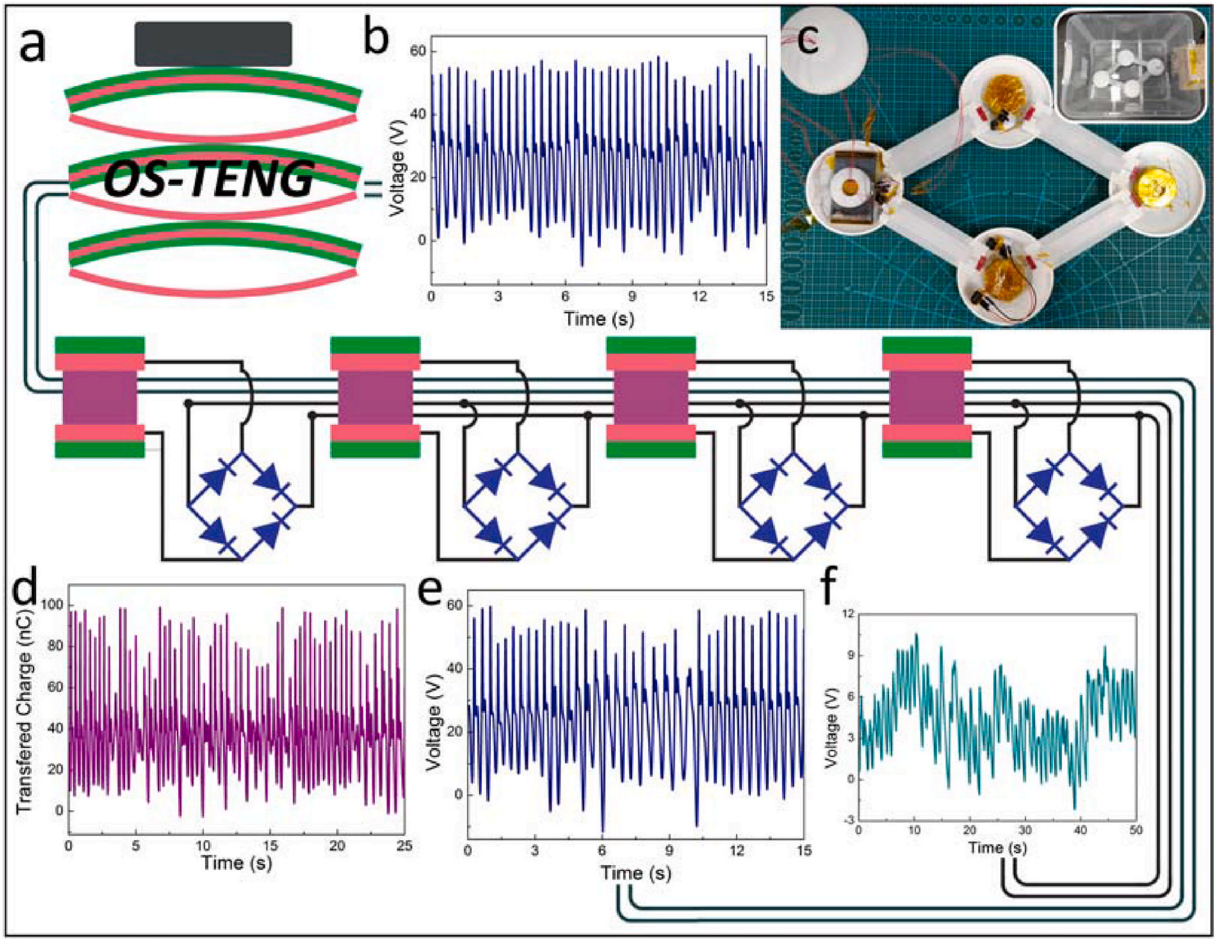

Fig. 5. Application of the power cable. a) Schematic diagram of the small TENG array. b) The output voltage of the OS-TENG through the straight-exit transmission wire. c) Photograph of the small TENG array before sealing and waterproofing. The inset shows the small TENG array working in a water tank. d) The transferred charge quantity and e) output voltage of the OS-TENG with its transmission wire passing through all four power cables. f) Output voltage of the four power cables with the array working in the water tank.

liquid-solid contact with water, producing electricity and enhancing the output performance of the overall TENG network. The influence of water on electric power transmission through various wires was studied experimentally, in order to obtain a thorough understanding of the importance of the power cable as a specially-made connecting device. The output behavior under different conditions was also investigated to explore the effect of water waves on the cable. A maximum open-circuit voltage of 34 V and a transferred charge quantity of 25 nC were achieved in one period for a single power cable. A small TENG array was assembled and connected by power cables for an over-water test. The power cables can maintain the rhomboid structure firmly and protect the output electricity of an OS-TENG without obvious decrease in output, suggesting that this design has considerable possibilities in large-scale TENG networks for blue energy harvesting.

4. Experimental Section

Fabrication of the triboelectric power cable. An 80 μm spring steel tape (Kobetool, Germany) was cut into slices 12 cm long and 2 cm wide using a paper cutter, followed by an alcohol rinse to remove oil contamination. A PET film with dimensions of 15 cm*4 cm*200 μm and two PTFE films with identical area and thickness of 80 μm were also prepared. A steel tape connecting a copper wire was stuck in the middle of the PET film using mucilage glue, as shown in Fig. 1c. The conducting wires to be sheltered were placed between the PET film and the steel tape before gluing. Then, mucilage glue was applied to the PET film around the steel tape to attach to the PTFE film. The above process was conducted on the other side of the PET film, thus creating a power cable with a symmetrical ribbon-like structure.

Fabrication of the Small Array. The hemi-oblate spheroidal shells in Fig. 5c and Fig. S15 were made of polylactic acid (PLA) using a 3D printer based on the same parameters in ref. 29: 23 mm height, 120 mm diameter, and ~3 mm wall thickness. The TENG in the array was also as described in ref. 29. The clump weight added to the shells was approximately 120 g. Four power cables were clamped between the hemi-oblate spheroidal shells by hot melt adhesive and then all shells were sealed for waterproofing.

Electrical Characterization. The open-circuit voltage and transferred charge were measured by a Keithley 6514 system electrometer. A linear motor (WMU1536075-090-D) provided a sinusoidal motion for the wave pool and the output measurement of power cable. The salt water for simulating seawater was a NaCl solution with mass fraction of 3.5%. For the bending test in Fig. 3d, the power cable was fixed on a bench clamp and the probe of a forcemeter (Weidu, WD-10) bent the power cable slowly in two directions successively. The distance between the catchpoint of the bench clamp and the contact point of the probe was 8 cm.

Declaration of competing interest

The authors declare that they have no known competing financial interests or personal relationships that could have appeared to influence the work reported in this paper.

CRediT authorship contribution statement

Guanlin Liu: Conceptualization, Methodology, Data curation, Writing - original draft, Writing - review & editing. **Longfa Xiao:** Formal analysis, Writing - review & editing. **Chaoyu Chen:** Validation, Resources. **Wenlin Liu:** Validation, Methodology. **Xianjie Pu:** Software, Data curation. **Zhiyi Wu:** Software, Resources. **Chenguo Hu:** Writing - original draft, Writing - review & editing, Supervision. **Zhong Lin Wang:** Conceptualization, Writing - original draft, Supervision.

Acknowledgements

The research is supported by the Fundamental Research Funds for the Central Universities (2019CDXZWL001, China), and the National Natural Science Foundation of China (51902035, 51772036), and Natural Science Foundation Project of Chongqing (cstc2019jcyj-msxmX0068).

Appendix A. Supplementary data

Supplementary data to this article can be found online at https://doi.org/10.1016/j.nanoen.2020.104975.

References

[1] A.S. Bahaj, Renew. Sustain. Energy Rev. 15 (2011) 3399.
[2] M. Penalba, J.V. Ringwood, Energies 9 (2016) 506.
[3] A. Siria, M.-L. Bocquet, L. Bocquet, Nat. Rev. Chem. 1 (2017) unsp. 0091.
[4] B. Czech, P. Bauer, IEEE Ind. Electron. Mag. 6 (2012) 4.
[5] F.R. Fan, Z. Tian, Z.L. Wang, Nano Energy 1 (2012) 328.
[6] Z.L. Wang, A.C. Wang, Mater. Today 30 (2019) 34.
[7] C. Wu, A.C. Wang, W. Ding, H. Guo, Z.L. Wang, Adv. Energy Mater. 9 (2019) 1802906.
[8] W. Ding, A.C. Wang, C. Wu, H. Guo, Z.L. Wang, Adv. Mater. Technol. 4 (2019) 1800487.
[9] Z. Lin, B. Zhang, H. Guo, Z. Wu, H. Zou, J. Yang, Z.L. Wang, Nano Energy 64 (2019) unsp. 103908.
[10] J. Wang, Z. Wu, L. Pan, R. Gao, B. Zhang, L. Yang, H. Guo, R. Liao, Z.L. Wang, ACS Nano 13 (2019) 2587.
[11] Z. Wu, B. Zhang, H. Zou, Z. Lin, G. Liu, Z.L. Wang, Adv. Energy Mater. 9 (2019) 1901124.
[12] B. Zhang, J. Chen, L. Jin, W. Deng, L. Zhang, H. Zhang, M. Zhu, W. Yang, Z. L. Wang, ACS Nano 10 (2016) 6241.
[13] B. Zhang, L. Zhang, W. Deng, L. Jin, F. Chun, H. Pan, B. Gu, H. Zhang, Z. Lv, W. Yang, Z.L. Wang, ACS Nano 11 (2017) 7440.
[14] L. Zhang, B. Zhang, J. Chen, L. Jin, W. Deng, J. Tang, H. Zhang, H. Pan, M. Zhu, W. Yang, Z.L. Wang, Adv. Mater. 28 (2016) 1650.
[15] J. Cheng, W. Ding, Y. Zi, Y. Lu, L. Ji, F. Liu, C. Wu, Z.L. Wang, Nat. Commun. 9 (2018) 3733.
[16] A. Li, Y. Zi, H. Guo, Z.L. Wang, F.M. Fernandez, Nat. Nanotechnol. 12 (2017) 481.
[17] Y. Bai, C. Han, C. He, G. Gu, J. Nie, J. Shao, T. Xiao, C. Deng, Z.L. Wang, Adv. Funct. Mater. 28 (2018) 1706680.
[18] J. Nie, Z. Ren, J. Shao, C. Deng, L. Xu, X. Chen, M. Li, Z.L. Wang, ACS Nano 12 (2018) 1491.
[19] G. Liu, J. Chen, Q. Tang, L. Feng, H. Yang, J. Li, Y. Xi, X. Wang, C. Hu, Adv. Energy Mater. 8 (2018) 1703086.
[20] R. Hinchet, H.-J. Yoon, H. Ryu, M.-K. Kim, E.-K. Choi, D.-S. Kim, S.-W. Kim, Science 365 (2019) 491.
[21] Z.L. Wang, Nature 542 (2017) 159.
[22] L. Xu, T. Jiang, P. Lin, J. Shao, C. He, W. Zhong, X. Chen, Z.L. Wang, ACS Nano 12 (2018) 1849.
[23] X. Hang, T. Jiang, G. Liu, T. Xiao, L. Xu, W. Li, F. Xi, C. Zhang, Z.L. Wang, Adv. Funct. Mater. 29 (2019) 1807241.
[24] X. Li, J. Tao, X. Wang, J. Zhu, C. Pan, Z.L. Wang, Adv. Energy Mater. 8 (2018) 1800705.
[25] S. Lee, J. Chung, D.Y. Kim, J.-Y. Jung, S.H. Lee, S. Lee, ACS Appl. Mater. Interfaces 8 (2016) 25014.
[26] J. Chen, J. Yang, Z. Li, X. Fan, Y. Zi, Q. Jing, H. Guo, Z. Wen, K. Pradel, S. Niu, Z. L. Wang, ACS Nano 9 (2015) 3324.
[27] W. Zhong, L. Xu, H. Wang, J. An, Z.L. Wang, Adv. Funct. Mater. 29 (2019), https://doi.org/10.1002/adfm.201905319.
[28] S. Zhang, M. Xu, C. Zhang, Y.-C. Wang, H. Zou, X. He, Z. Wang, Z.L. Wang, Nano Energy 48 (2018) 421.
[29] G. Liu, H. Guo, S. Xu, C. Hu, Z.L. Wang, Adv. Energy Mater. 9 (2019) 1900801.
[30] Z.-H. Lin, G. Cheng, S.M. Lee, K.C. Pradel, Z.L. Wang, Adv. Mater. 26 (2014) 4690.
[31] X. Zhao, S. Kuang, Z.L. Wang, G. Zhu, ACS Nano 12 (2018) 4280.
[32] H. Zou, Y. Zhang, L. Guo, P. Wang, X. He, G. Dai, H. Zheng, C. Chen, A. Wang, C. Xu, Z.L. Wang, Nat. Commun. 10 (2019) 1427.
[33] Y. Zhang, H. Sun, C.K. Jeong, ACS Appl. Mater. Interfaces 10 (2018) 35539.
[34] B.Y. Lee, D.H. Kim, J. Park, K. Park, K.J. Lee, C.K. Jeong, Sci. Technol. Adv. Mater. 20 (2019) 758.
[35] J. Nie, Z. Ren, L. Xu, S. Lin, F. Zhan, X. Chen, Z.L. Wang, Adv. Mater. 32 (2020) 1905696.
[36] S. Lin, L. Xu, A.C. Wang, Z.L. Wang, Nat. Commun. 11 (2020) 399.

Guanlin Liu received B.S. degree (2014) Ph.D. degree (2019) in Physics from Chongqing University. He was a visiting Ph.D. student at Georgia Institute of Technology through the program of China Scholarship Council, and now is an associate professor of Physics at Guangxi University. His current research interest is triboelectric nanogenerator for blue energy harvesting.

Longfa Xiao is a master student of Materials Science and Engineering from the School of Resources, Environment and Materials at the Guangxi University. He received his bachelor's degree in Materials Processing and Control Engineering from Inner Mongolia University of Science and Technology in 2016. His current research focus on the application of triboelectric nanogenerator networks for large-scale blue energy harvesting.

Chaoyu Chen is a Ph.D. student under the supervision of Prof. Zhaoqun Du and Prof. Weidong Yu in College of Textile, Donghua University. His research interests are in spacer fabric, textile based triboelectric nanogenerators, and self-powered sensors.

Wenlin Liu received his B.S. degree in Applied Physics (2017) from Chongqing University. Now, he is a Ph.D. student in Chongqing University. His research interests are mainly focused on triboelectric nanogenerator.

Xianjie Pu received her B.S. degree in Biomedical Engineering from Chongqing University (CQU) in 2008 and M.S. degree in Biomedical Engineering from UESTC in 2011. She has been a faculty member of TMMU (2011–2014) and CQU (2014). She is currently pursuing the Ph.D. degree with the Department of Applied Physics, CQU. Her current interests include self-powered sensors, systems and applications based on nanogenerators.

Zhiyi Wu received Ph.D. degree in Instrument Science and Technology from Chongqing University in 2013. He is now a researcher in Beijing Institute of Nanoenergy and Nanosystems, Chinese Academy of Sciences. His current research focuses on the Nanoenergy and self-powered sensors.

Chenguo Hu is a professor of physics in Chongqing University and the director of Key Lab of Materials Physics of Chongqing Municipality. She received her Ph.D. from Chongqing University in 2003. Her research interests include the investigation of morphology and size dependent physical and chemical properties of nanomaterials, and design and fabrication of electronic devices, such as nanogenerators and self-powered sensors.

Zhong Lin Wang is a Hightower Chair and Regents's Professor at Georgia Tech. He is also the Chief scientist and Director for the Beijing Institute of Nanoenergy and Nanosystems, Chinese Academy of Sciences. His discovery and breakthroughs in developing nanogenerators establish the principle and technological road map for harvesting mechanical energy from environmental and biological systems for powering personal electronics. He coined and pioneered the field of piezotronics and piezo-phototronics by introducing piezoelectric potential gated charge transport process in fabricating new electronic and optoelectronic devices.